Nanotechnology

DOI: 10.1002/anie.200905200

Targeted Optimization of a Protein Nanomachine for Operation in Biohybrid Devices**

*Mamta Amrute-Nayak, Ralph P. Diensthuber, Walter Steffen, Daniela Kathmann, Falk K. Hartmann, Roman Fedorov, Claus Urbanke, Dietmar J. Manstein, Bernhard Brenner, and Georgios Tsiavaliaris**

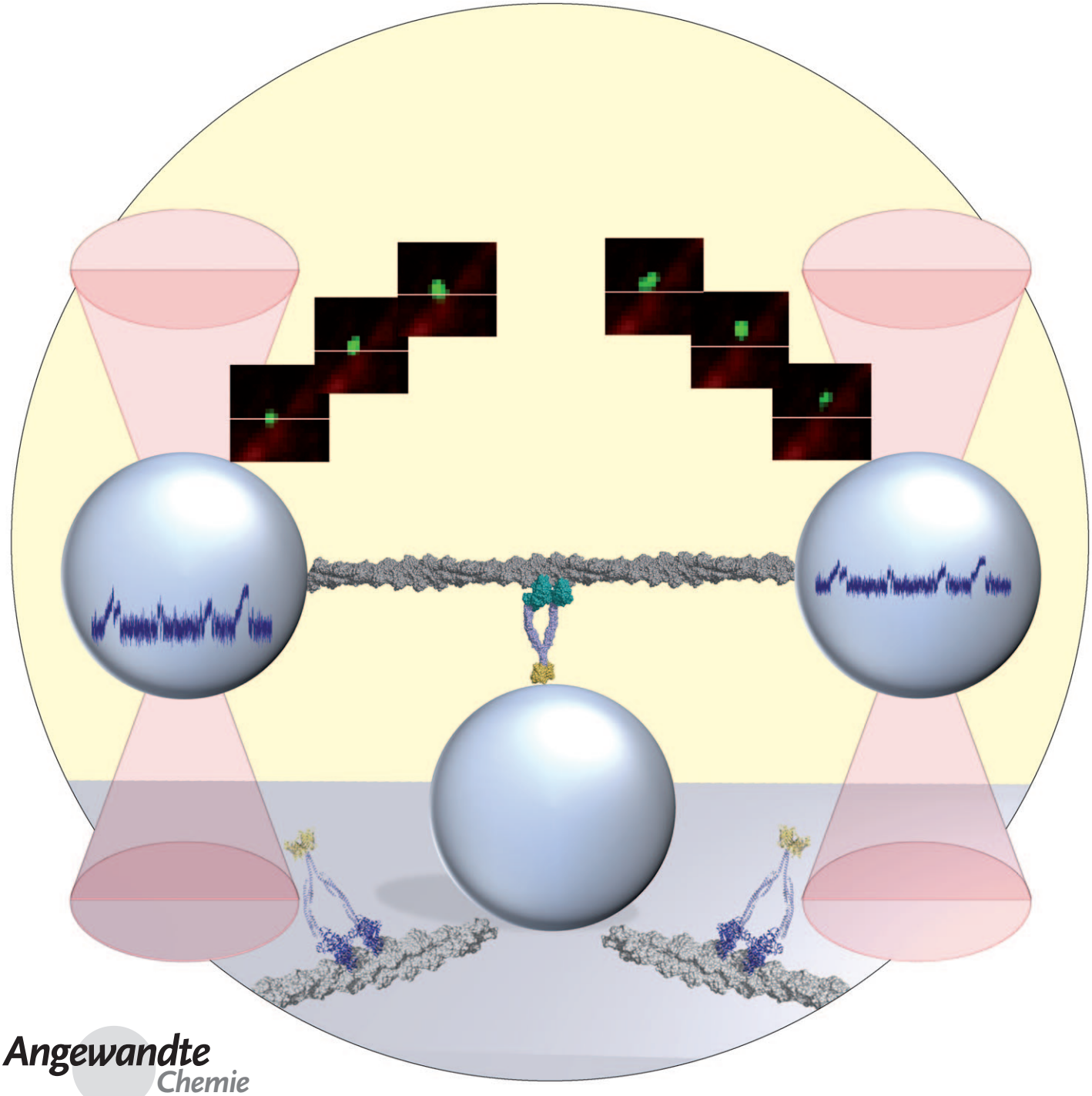

Owing to their ability to convert chemical energy into mechanical work and directed movement, motor proteins of the myosin and kinesin families—along with their polymeric tracks, F-actin and microtubules—are of particular interest as biomechanical force transducers and actuators in synthetic environments.[1–5] Motor proteins hold additional potential for sorting, sensing, and assembly functions in lab-on-a-chip applications.[6,7] Such functions can be implemented in biohybrid devices in which a) the motor protein is attached to the surface and moves the polymeric tracks[8,9] or b) the tracks themselves are immobilized on a surface, and single motors shuttle cargo along these tracks.[10,11] Processive class-5 myosins, which move in a hand-over-hand fashion several hundred nanometers along actin filaments without dissociating, are excellent candidates for the powering of nanoscale transport processes, especially in the latter configuration.[12,13] Their modular structure formed by a globular motor domain, an extended neck region with bound light chains, and a versatile tail domain facilitates their functional manipulation.[14] Protein-engineering tools have been successfully employed to generate myosin constructs with altered substrate specificity,[15] increased or decreased enzymatic and motile activity,[16] or reversed directionality of movement.[17] The construction of functional biohybrid structures with myosins as integral components is, however, hindered by the limited stability of the proteins outside of their cellular environment and the difficulty of accurately controlling and regulating the motor-driven transport processes.

Herein, we describe a structure-based molecular-engineering approach that led to the design and generation of two myosin constructs: dimeric M5P (processive myosin-5) and monomeric M5S (single-headed myosin-5), which displayed switchable processivity and tight control of the velocity of movement, respectively. Both constructs contain the myosin-5b motor domain from *Dictyostelium discoideum*. We previously characterized this myosin-5b domain as a conditional processive motor with motor properties that can be modulated by changes in the concentration of free Mg^{2+} ions ($[Mg^{2+}]_{free}$).[18] A 13 nm long rod-shaped domain composed of two α-actinin repeats and referred to as 2R was used as an artificial lever for both constructs.[19] In M5S, we engineered the actin-binding loop 2 (amino acids 647–683) in the motor domain to contain six consecutive GKK motifs, which form a flexible cluster of positive charges. Additional positive charges in this region were shown to increase actin affinity and coupling between actin and adenosine-5′-triphosphate (ATP) binding.[15] Since a dimeric structure is essential for processivity, we fused a leucine-zipper[20] dimerization domain (LZ) derived from the transcriptional activator GCN4 to the C terminus of M5P.

To further increase the stability of the dimer, we generated a model of M5P based on the structures of the individual building blocks.[19,21,22] By using molecular dynamics and energy-minimization procedures, we obtained the refined structural model of M5P shown in Figure 1a; the dimerization of M5P is strengthened by the introduction of the mutation Arg238Asp with the creation of an additional interchain interaction in the LZ segment (Figure 1b). Additionally, the interchain interaction between α-actinin residues Arg235 and Glu234 in the 2R building block contributes to dimer stability. Stable dimerization of M5P at micromolar concentrations was confirmed by sedimentation–diffusion equilibrium experiments (see Figure S1a in the Supporting Information). The experiments revealed a single population of molecules with an apparent molecular mass of $300 \pm 12\ kg\,mol^{-1}$, which agrees well with the calculated molecular mass of 307.3 kDa of M5P. To show that M5P remains dimeric at nanomolar concentrations, we performed photobleaching experiments (see Figure S1b in the Supporting Information). The fluorescence signal of individual molecules tagged with yellow fluorescent protein (YFP) disappeared in two distinct steps of similar amplitude. This behavior is indicative of the sequential photobleaching of two YFP moieties per M5P molecule and confirms the dimerization.

To examine whether M5P has sufficient internal flexibility to support processive movement along actin filaments, we computed the possible movements of the polypeptide chains in the dimer by normal-mode vibrational analysis.[23] The analysis was performed without the motor domain on the 2R–LZ module alone, since 2R–LZ is the structurally relevant element that needs to provide sufficient flexibility between the head fragments.[24] Two low-frequency modes describing the largest movements are shown in Figure 1c. The 2R–LZ structure displays a high degree of flexibility that is characterized by large scissoring (ca. 9 nm) and tilting (ca. 5 nm) movements around a hinge region located between the triple-helix repeats of the 2R fragments (Figure 1d). Animations describing the flexibility of 2R–LZ on the basis of six low-frequency modes are shown in the Supporting Information (movies M1 and M6). Taking into account the size of the motor domains and their ability to rotate freely around the junction with the 2R–LZ unit, we predicted that M5P would move in steps of up to 18 nm in length along actin filaments.

To verify the double-headed binding of M5P to F-actin experimentally, we investigated its interaction with pyrene-labeled F-actin by fluorescence-quenching experiments. The

[*] Dr. R. P. Diensthuber,[+] D. Kathmann, F. K. Hartmann, Dr. R. Fedorov, Prof. Dr. C. Urbanke, Prof. Dr. D. J. Manstein, Prof. Dr. G. Tsiavaliaris
Institut für Biophysikalische Chemie OE4350
Medizinische Hochschule Hannover
Carl-Neuberg-Strasse 1, 30623 Hannover (Germany)
Fax: (+49) 511-532-5966
E-mail: tsiavaliaris.georgios@mh-hannover.de
Homepage: http://www.mh-hannover.de/bpc_uncmyo.html
Dr. M. Amrute-Nayak,[+] Dr. W. Steffen, Prof. Dr. B. Brenner
Institut für Molekular- und Zellphysiologie OE4350
Medizinische Hochschule Hannover (Germany)

[+] These authors contributed equally.

[**] We thank Dr. M. H. Taft and Dr. I. Chizhov (MHH) for help and discussions, and C. Thiel and C. Waßmann (MHH) for excellent technical assistance. This research was supported by the Deutsche Forschungsgemeinschaft through grants TS169-2.1 (G.T. and D.J.M.), TS169-3.1 (G.T.), M1081/ (D.J.M.), ST1697/1 (W.S.), BR849/21-3, and BR849/29-1.2 (B.B.), by the Fonds der Chemischen Industrie (D.J.M.), and by the Österreichische Akademie der Wissenschaften (R.P.D.).

Supporting information for this article is available on the WWW under http://dx.doi.org/10.1002/anie.200905200.

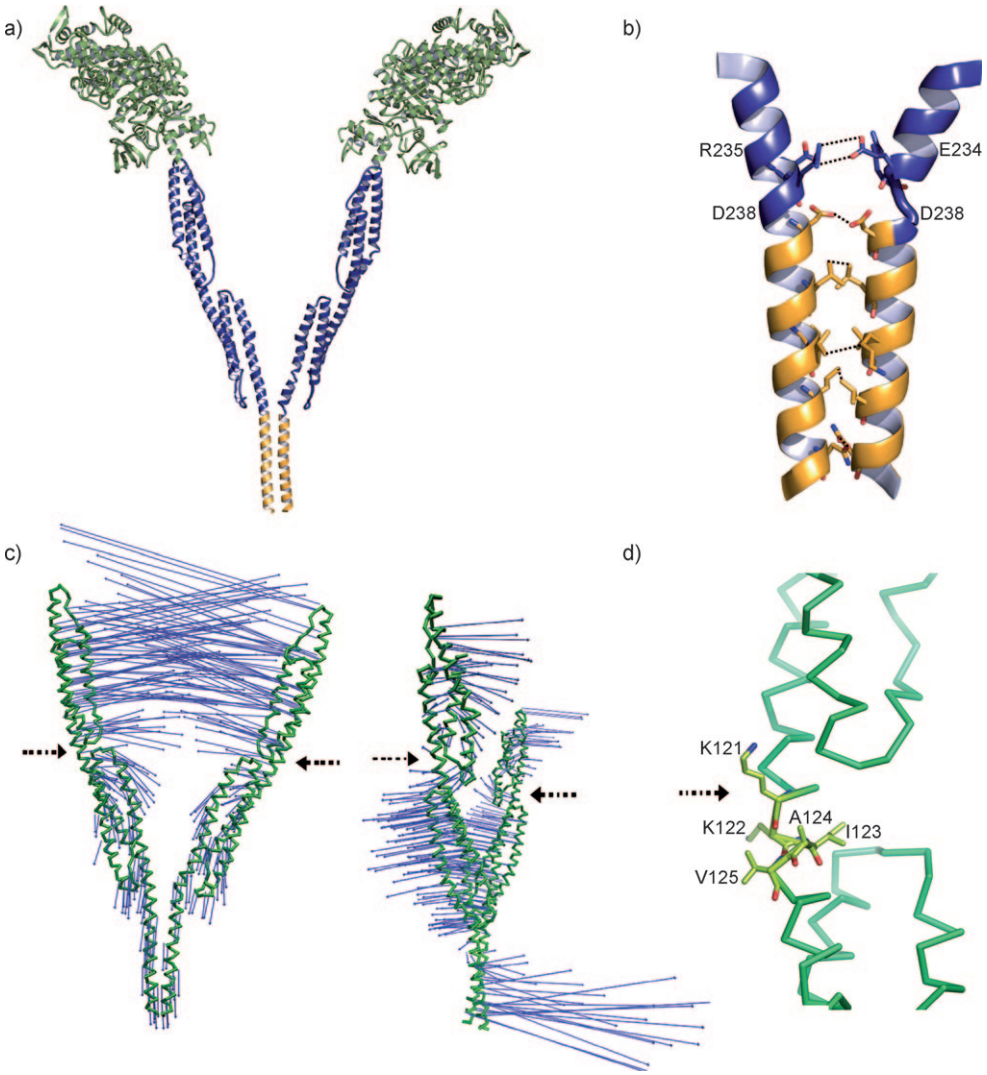

Figure 1. Molecular engineering of M5P. a) Structural model of M5P. The dimeric motor is composed of the myosin-5b motor domain (green), two α-actinin repeats (blue), and the GCN4 leucine-zipper motif (orange). b) Graphical representation of the helical junction between α-actinin (blue) and the leucine zipper (orange). Interchain interactions that strengthen dimer stability are highlighted. c) Normal-mode analysis of the 2R–LZ structure. The blue arrows indicate the direction vectors of movement for two different vibrational normal modes (left and right). The hinge region is indicated by the black arrows. d) Amino acids that form the hinge region are highlighted in light green.

maximum amplitude of the quenching reaction was observed at a stoichiometry of one M5P molecule to two actin monomers; this stoichiometry is indicative of two-headed binding to F-actin[25] (see Figure S1c in the Supporting Information). In direct tests for processive movement, we employed YFP-tagged M5P molecules in a single-molecule assay in which actin filaments labeled with Alexa 633 phalloidin were immobilized on the glass surface and single M5P molecules were bound to the actin filaments. Upon the addition of ATP (4 mM) and free Mg^{2+} ions (10 mM), single M5P molecules were observed to move along actin filaments. The distribution of run lengths (total distance moved) is best described by an exponential decay function with a length constant (L_p) of 700 ± 150 nm (Figure 2a). The observed run-length distribution reflects a typical processive run as observed for class-5 myosins: the motors stay associated to the actin filament for multiple steps, but on average not long enough to reach the end of the filament.[26]

Next, we examined the extent to which M5P motor activity can be modulated by changes in the concentration of free Mg^{2+} ions. At $[Mg^{2+}]_{free} < 0.5$ mM, processive runs were completely absent. At $[Mg^{2+}]_{free} = 10$ mM, the motor displayed exclusively processive behavior. We confirmed these $[Mg^{2+}]_{free}$-dependent changes in processivity as a result of changes in the lifetime of the motor in the strongly actin bound states by single-molecule dwell-time measurements[27] (see Figure S1e in the Supporting Information). At $[Mg^{2+}]_{free} = 4$ mM, the lifetime of the nucleotide-bound states was decreased fivefold ($\tau_{4\,mM} = 2.38 \pm 0.21$ s) relative to that at $[Mg^{2+}]_{free} = 10$ mM ($\tau_{10\,mM} = 12.1 \pm 0.85$ s). This result is consistent with a Mg^{2+}-dependent rate of ADP release, which determines the fraction of time the motor spends in the strong actin-binding states. These properties of M5P enable fast switching between processive and non-processive movement. A simple change in $[Mg^{2+}]_{free}$ in the surrounding assay buffer is sufficient to switch the mode of movement.

To study the processive movement of M5P in detail, we performed optical-trap experiments by using a two-bead actin-filament dumbbell configuration.[28] Single M5P molecules were observed to produce multiple staircaselike signals upon binding to F-actin. At low stiffness of the trap, the maximum displacement was 60 nm, which corresponds to a stall force of approximately 2 pN (Figure 2b). The individual steps within the staircases ranged from 4 to 17 nm with preferred step sizes of 5 ± 1.5 and 10 ± 1.5 nm (Figure 2c). These step sizes reflect the distance of the subunit repeats within the actin filament and agree with the results of our modeling studies, which predicted a maximum step size of 18 nm.

We generated the construct M5S to exploit additional means for the parametric control of myosin-motor activity. In the context of myosin-based biohybrid devices, it is advanta-

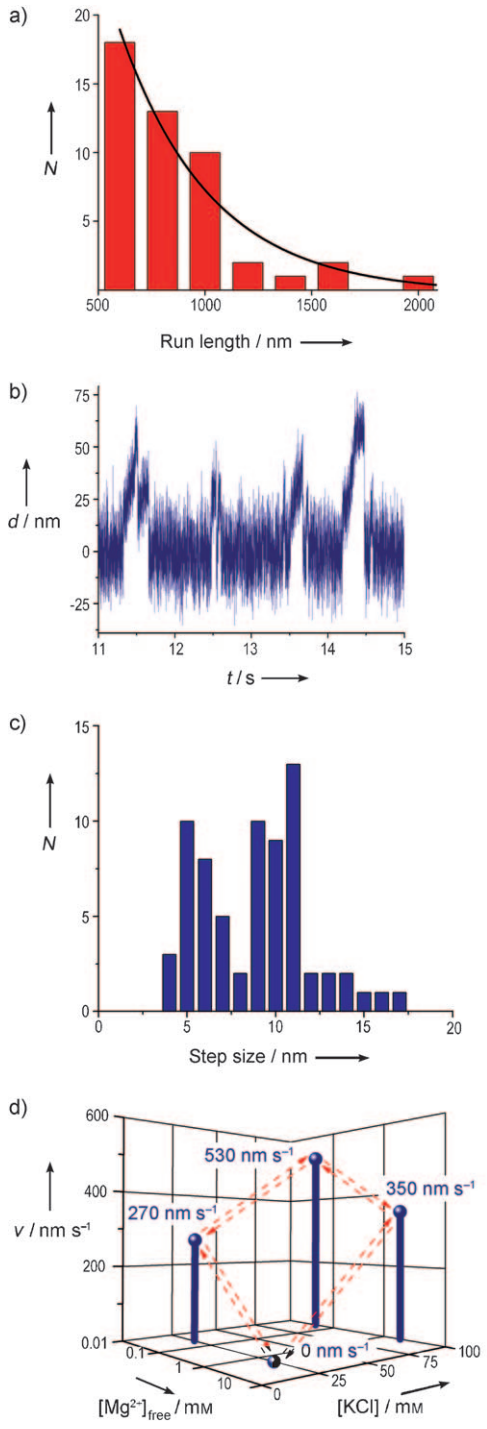

Figure 2. Analysis of processivity and motile activity. a) Run-length distribution for single, fluorescently labeled M5P molecules (N = number of events). The black curve is the best fit to the data with a single exponential function ($L_p = 700 \pm 150$ nm, $N_{total} = 47$). b) Sample trace from a two-bead laser-trap experiment of the stepping behavior of a single M5P molecule at an ATP concentration of 1 mM and $[Mg^{2+}]_{free} = 4$ mM. The motor showed repeated processive runs up to a stall force of approximately 2 pN. c) Histogram showing the statistical distribution of step sizes during processive movement ($N_{total} = 68$). d) Control of the motile activity of M5S by the combined effect of changes in the concentration of free Mg^{2+} ions and KCl. Experiments in which the same flow cell was used show that the switching between the motile and nonmotile states is reversible (dashed red arrows).

geous to have the ability to induce two types of changes in motile activity: gradual adjustments in the velocity of movement and the complete switching of motor activity between on and off states. Previously, we showed that the engineering of loop-2 affects the ionic-strength-dependent interaction of myosin with F-actin.[15] In generating construct M5S, we took advantage of this behavior by introducing an engineered lysine-rich loop-2. The motile activity of the resulting construct was expected to feature the $[Mg^{2+}]_{free}$ dependence of the native myosin-5 motor domain in combination with increased sensitivity to changes in ionic strength. The predicted changes in the ionic-environment-dependent motile properties of M5S were verified with an in vitro gliding actin filament assay.[8] The results summarized in Figure 2d show how changes in the ion composition of the assay buffer can be used to fine-tune the activity of the motor protein. Both changes induced by altering $[Mg^{2+}]_{free}$ and [KCl] were shown to occur independently from changes in [ATP]. In the presence of ATP (4 mM) and KCl (25 mM) at $[Mg^{2+}]_{free} = 1.9$ mM, the actin filaments form a stable complex with surface-attached M5S but are not translocated by the engineered motor protein. The maximum motile activity of M5S was observed following a 50-fold reduction in $[Mg^{2+}]_{free}$ to 0.04 mM in combination with a fourfold increase in [KCl] to 100 mM. We observed well-defined, gradual, and reversible transitions between immobility and the maximum velocity of M5S-supported F-actin sliding upon alteration of the [KCl]/$[Mg^{2+}]_{free}$ ratio within the concentration range indicated in Figure 2d.

In comparison to the class-1 and class-2 myosin constructs that we tested previously,[29–31] M5P and M5S are characterized by substantially greater stability in solution and in the surface-attached state. The engineered constructs can be stored with minimal loss of motor activity for at least 3 months at 4 °C in solution. Following the storage of assay chambers with surface-bound M5S at 4 °C over a period of 7 days, more than 60 % of actin filaments were translocated with the same velocity as that observed with the freshly decorated assay chambers. In comparison, a myosin-2 motor-domain construct with an artificial lever[29] displayed only approximately 10 % of its initial motor activity after storage for 2 days at 4 °C, and no motile activity was detectable after 3 days (see Figure S1f in the Supporting Information).

The requirements for an effective and general implementation of biological transport in a biohybrid device include a high level of stability of the biological components, the ability to modify the biological components accurately, and straightforward control of the transport processes. Current implementations of external control mechanisms for motor-protein-mediated transport processes[32–35] are in most instances complementary and compatible with the approach described herein. Additionally, our results show how structure-based engineering facilitates the task of optimizing the properties of a molecular motor in terms of the ease with which the functional states of motor-protein-based biohybrid devices can be altered and the extent to which the useful lifetime of such devices can be prolonged.[36] The simple parametric control that is possible with our engineered motors is important for the generation of biohybrid microdevices with

applications ranging from the organization of directed transport with the targeted accumulation of cargo to assembly and sensing functions.[6,37]

Received: September 16, 2009
Published online: November 17, 2009

Keywords: biohybrid devices · molecular modeling · motor proteins · movement · protein engineering

[1] C. Brunner, C. Wahnes, V. Vogel, *Lab Chip* **2007**, *7*, 1263.
[2] H. Hess, G. D. Bachand, V. Vogel, *Chem. Eur. J.* **2004**, *10*, 2110.
[3] D. Spetzler, J. York, C. Dobbin, J. Martin, R. Ishmukhametov, L. Day, J. Yu, H. Kang, K. Porter, T. Hornung, W. D. Frasch, *Lab Chip* **2007**, *7*, 1633.
[4] M. Sundberg, R. Bunk, N. Albet-Torres, A. Kvennefors, F. Persson, L. Montelius, I. A. Nicholls, S. Ghatnekar-Nilsson, P. Omling, S. Tågerud, A. Månsson, *Langmuir* **2006**, *22*, 7286.
[5] H. Hess, V. Vogel, *J. Biotechnol.* **2001**, *82*, 67.
[6] A. Goel, V. Vogel, *Nat. Nanotechnol.* **2008**, *3*, 465.
[7] M. G. van den Heuvel, C. Dekker, *Science* **2007**, *317*, 333.
[8] S. J. Kron, J. A. Spudich, *Proc. Natl. Acad. Sci. USA* **1986**, *83*, 6272.
[9] J. Howard, A. J. Hudspeth, R. D. Vale, *Nature* **1989**, *342*, 154.
[10] J. T. Finer, R. M. Simmons, J. A. Spudich, *Nature* **1994**, *368*, 113.
[11] S. M. Block, L. S. Goldstein, B. J. Schnapp, *Nature* **1990**, *348*, 348.
[12] T. Sakamoto, I. Amitani, E. Yokota, T. Ando, *Biochem. Biophys. Res. Commun.* **2000**, *272*, 586.
[13] A. Yildiz, J. N. Forkey, S. A. McKinney, T. Ha, Y. E. Goldman, P. R. Selvin, *Science* **2003**, *300*, 2061.
[14] D. J. Manstein, *Philos. Trans. R. Soc. London Ser. B* **2004**, *359*, 1907.
[15] M. Furch, M. A. Geeves, D. J. Manstein, *Biochemistry* **1998**, *37*, 6317.
[16] C. Ruff, M. Furch, B. Brenner, D. J. Manstein, E. Meyhofer, *Nat. Struct. Biol.* **2001**, *8*, 226.
[17] G. Tsiavaliaris, S. Fujita-Becker, D. J. Manstein, *Nature* **2004**, *427*, 558.
[18] M. H. Taft, F. K. Hartmann, A. Rump, H. Keller, I. Chizhov, D. J. Manstein, G. Tsiavaliaris, *J. Biol. Chem.* **2008**, *283*, 26902.
[19] W. Kliche, S. Fujita-Becker, M. Kollmar, D. J. Manstein, F. J. Kull, *EMBO J.* **2001**, *20*, 40.
[20] W. H. Landschulz, P. F. Johnson, S. L. McKnight, *Science* **1988**, *240*, 1759.
[21] P. D. Coureux, A. L. Wells, J. Menetrey, C. M. Yengo, C. A. Morris, H. L. Sweeney, A. Houdusse, *Nature* **2003**, *425*, 419.
[22] E. K. O'Shea, J. D. Klemm, P. S. Kim, T. Alber, *Science* **1991**, *254*, 539.
[23] S. M. Hollup, G. Salensminde, N. Reuter, *BMC Bioinf.* **2005**, *6*, 52.
[24] T. J. Purcell, C. Morris, J. A. Spudich, H. L. Sweeney, *Proc. Natl. Acad. Sci. USA* **2002**, *99*, 14159.
[25] T. Chakrabarty, C. Yengo, C. Baldacchino, L. Q. Chen, H. L. Sweeney, P. R. Selvin, *Biochemistry* **2003**, *42*, 12886.
[26] T. Sakamoto, F. Wang, S. Schmitz, Y. Xu, Q. Xu, J. E. Molloy, C. Veigel, J. R. Sellers, *J. Biol. Chem.* **2003**, *278*, 29201.
[27] M. Amrute-Nayak, M. Antognozzi, T. Scholz, H. Kojima, B. Brenner, *J. Biol. Chem.* **2008**, *283*, 3773.
[28] W. Steffen, D. Smith, R. Simmons, J. Sleep, *Proc. Natl. Acad. Sci. USA* **2001**, *98*, 14949.
[29] M. Anson, M. A. Geeves, S. E. Kurzawa, D. J. Manstein, *EMBO J.* **1996**, *15*, 6069.
[30] S. Fujita-Becker, U. Dürrwang, M. Erent, R. J. Clark, M. A. Geeves, D. J. Manstein, *J. Biol. Chem.* **2005**, *280*, 6064.
[31] G. Tsiavaliaris, S. Fujita-Becker, U. Durrwang, R. P. Diensthuber, M. A. Geeves, D. J. Manstein, *J. Biol. Chem.* **2008**, *283*, 4520.
[32] H. Higuchi, E. Muto, Y. Inoue, T. Yanagida, *Proc. Natl. Acad. Sci. USA* **1997**, *94*, 4395.
[33] B. M. Hutchins, M. Platt, W. O. Hancock, M. E. Williams, *Small* **2007**, *3*, 126.
[34] L. Ionov, M. Stamm, S. Diez, *Nano Lett.* **2006**, *6*, 1982.
[35] M. G. van den Heuvel, M. P. de Graaff, C. Dekker, *Science* **2006**, *312*, 910.
[36] R. Seetharam, Y. Wada, S. Ramachandran, H. Hess, P. Satir, *Lab Chip* **2006**, *6*, 1239.
[37] H. Hess, J. Clemmens, C. Brunner, R. Doot, S. Luna, K. H. Ernst, V. Vogel, *Nano Lett.* **2005**, *5*, 629.

